PAPER • OPEN ACCESS

Novel Bio-compatible Tracers for Positron Emission Particle Tracking

View the article online for updates and enhancements.

Novel Bio-compatible Tracers for Positron Emission Particle Tracking

Yu-Fen Chang[1,2,3] and Boris V. Balakin[2]

[1] Department of Clinical Medicine, UiT The Arctic University of Norway, Norway
[2] Western Norway University of Applied Sciences, Norway
[3] University Hospital of North Norway, Norway

Yu-Fen.Chang@uit.no

Abstract. To study the flow of objects in opaque flow processes, the PEPT (positron emission particle tracking) technique may be utilized. The PEPT technique is based on the same principle of positron emission tomography (PET). Both techniques detect the characteristic back-to-back gamma pairs caused by positron-electron annihilation. PEPT allows tracking of β+ - activated objects (tracers) with high spatial (microns) and temporal resolutions (milliseconds). This makes the technique promising in a number of medical applications that require observation of fast transient phenomena e.g. heart and brain hemodynamics, the aerodynamics of respiratory tract etc. However, a majority of PEPT-tracers used nowadays are tailored for industrial applications and are based on solid particles of a micrometric size, which are hardly suitable for *in-vivo* tests. In this contribution, we propose new bio-compatible tracers. The tracers are based on frozen radioactive solutions rather than activated solids. We produced a number of millimetre-sized ice tracers dispersing the droplets of radioactive solution in oil at negative temperatures. In this preliminary study, we demonstrate how the tracers behave in a settling column and in an agitated vessel. The PEPT-tracks are presented together with a supplementary numerical analysis that was conducted in order to estimate the freezing time of the droplets.

1. Introduction

Positron-emitting isotopes such as ^{18}F, ^{68}Ga, ^{13}N, and ^{11}C have been utilized to activate tracers for positron emission tomography (PET) via chemical bonding. The positron, after emitted from the isotope, travels a finite distance before annihilating with an electron. For example, the average distance of positrons in water emanated from ^{18}F, ^{68}Ga, ^{13}N, and ^{11}C are 0.6 mm, 2.9 mm, 1.5 mm, and 1.1 mm, respectively [1]. The positron-electron annihilation results in a pair of back-to-back 511-keV gamma rays.

Conventional PET scanners consist of position-sensitive gamma detectors or gamma detector matrices for identifying the gamma pairs if they are detected within a short time window and within a predefined energy range. Specialised image reconstruction methods are employed to process the lines of response (LORs) connecting the detector pairs, producing 3D distribution of the radioactive compounds and intensity maps. The temporal resolutions of the contemporary dynamic PET scans are at the scale of more than a few seconds, which is sufficient for detecting many biological processes. However, the current temporal resolutions pose limitations on detecting dynamic processes with high velocities, such as blood flow. The temporal and spatial resolutions are intercorrelated, and both are affected by signal statistics, scanner construction, and data processing algorithms.

To address the limitations of the temporal and spatial resolutions of the conventional PET in medical applications, in this work we proposed to further develop the positron emission particle tracking (PEPT) technique as well as to develop bio-compatible PEPT tracers. The PEPT technique is based on the same principle of PET in terms of detecting the characteristic back-to-back gamma pairs originated from positron-electron annihilation. However, since the tracers are used to reflect the high-velocity processes, point-like individual tracer particles are employed. In addition, in order to achieve tracking of tracers with spatial and temporal resolutions higher than PET, the data processing algorithms have to be re-designed and developed separately. Several innovative approaches (see, e.g., [2,3]), including methods involving machine learning [4], have been proposed and refined in the last decade. A number of algorithms have been developed by the PEPT research cluster in Norway [3,5] and applied to study complex, turbulent flow patterns in industrial processes and multiphase flow in equipment (e.g. [5-7]).

For investigating flow in process equipment using PEPT, the biological toxicity of the tracer particles are not of concern, and therefore materials such as ion exchange resins have been employed in order to optimise radionuclide absorption and be able to represent the flow of studied subjects [3,8]. To further develop the PEPT technique for medical applications, the bio-compatibility of the tracers needs to be taken into consideration. In this work, we explored the possibility of using frozen droplets (i.e. ice particles) as PEPT tracers, in the expectation that frozen droplets of bio-compatible liquids as tracers will further open up the potential of applying PEPT as a diagnostic and even a theranostic tool.

2. Materials and methods

2.1 The tracer particles and the carrier liquid

Positron-emitting radioactive solutions for making ice particles were produced in the Tromsø PET Imaging Center, University Hospital of North Norway. The water solution containing ^{18}F and the ammonia solution with ^{13}N were produced in a cyclotron from GE Healthcare. The solution of $^{68}GaCl_3$ was produced by ^{68}Ga generator GalliAd (IRE-ELiT S.A.).

Radioactive droplets were dispensed by the micropipette (Eppendorf) in linseed oil (Helios). Linseed oil is chosen as the carrier medium for radioactive droplets in this study as the radioactive solution is immiscible with the oil and the oil has a low melting point at around -20 °C. The density of linseed oil between -10 °C and 0 °C is estimated around 947 kg/m^3 and around 940 kg/m^3 between 0 °C and 10 °C. The linseed oil is stored at -18 °C before the experiments.

2.2 Gamma-ray detector matrix

The preclinical PET camera LabPET8 (TriFoil Imaging Inc.), was used as the gamma-ray detector matrix. The LabPET8 consists of 3072 phoswich detectors surrounding a cylindrical space of diameter 162 mm and axial length 75 mm. Each phoswich detector is composed of two trapezoidally shaped scintillators of two different crystals, LYSO (lutetium-yttrium oxyorthosilicate) and LGSO (lutetium-gadolinium oxyorthosilicate), making up a total of 6144 crystals. The cross-section of each crystal is 2 × 2 mm^2, and the mean lengths of the side-by-side optically coupled LYSO and LGSO crystals are 11 mm and 13 mm, respectively. Each phoswich pair is read out by a single avalanche photodiode (APD). More details about the detectors, construction, and electronics can be found in LabPET related literature (e.g. [9]). Information from the detector pairs was recorded in the list mode format, i.e. as a sequential list of entries. A timestamp was inserted into the data stream every 5.2 ms.

2.3 Particle positioning and data processing

When back-to-back gamma pairs were detected, the events were stored in list-mode format containing the information of detector positions. The algorithms for tracking droplets and ice particles used in this study were based on the same principle developed in [3] and refined for the specific gamma-ray detector matrix. The analysis started from finding the 2D cross-points of all LORs which were defined by each detector pair. After a few iterative de-noising steps, the average of the "most likely true" cross-points within an optimised spatial window were obtained. The average of the cross-points on the third axis was

obtained by processing the LORs left from the previous de-noising steps. This process was carried out for consecutive time periods until a user-defined criterion was met, after which the method only processed cross-points that were around the previously found position. This way, the efficiency and accuracy of positioning were both increased compared to processing all cross-points in the entire field of view (FOV) of the scanner. In the data stream, timestamps were inserted every 5.2 ms by the LabPET8 machine. Data of each machine-timestamped interval can be combined or split to achieve different temporal resolutions. The above-described data processing algorithms were implemented in-house using the programming language Fortran.

3. Experiments

3.1 Radioactive droplets in static oil column

The linseed oil contained in 15 ml centrifuge tubes (SuperClear, VWR) were stored in a -18 °C freezer before experiments. Several volumes of radioactive solution within the interval 5–10 μl were dropped into stationary linseed oil of different temperatures between -18 °C and 10 °C. In order to verify the solidification of droplets, a supplementary CFD-model of the process was developed in the commercial code STAR-CCM+. The model utilizes a standard melting-solidification model of the code [10]. In this model, the ice substitutes a porous resistance that hinders the flow of the liquid phase. The energy equation of the ice-liquid system includes the source term originating from the latent heat of ice formation. The volume of the droplet was discretized with 100-μm polyhedral cells in the core of the drop and 7-μm prismatic cells at the boundary (see Fig.2). The Neumann-type boundary condition is set at the surface of the droplet, the coefficient of heat transfer is given using the Ranz-Marshall [11] correlation where the velocity of the drop in the oil is presented by a passive scalar.

3.2 Radioactive ice particles in mixer

The water droplets activated with ^{18}F (0.5 μl and 3 μl) were dropped in linseed oil contained in 50 ml centrifugal tubes. The tubes together with the radioactive droplets were then refrozen in -80 °C until one third of the oil in the tube became solidified. As a part of the linseed oil in the tube was frozen, the average temperature in the tube was established between -16 °C and -24 °C. Afterward, the tube containing the radioactive drop together with other 1/3 frozen oil tubes were poured into a mixer (Portable Blender, BlendJet). This procedure was to ensure the formation of an ice particle as the mixer was turned on. Around 50% of the mixer space contained oil. Once turned on, the mixer automatically stopped after 40 seconds.

4. Results and discussion

4.1 Radioactive droplets in static oil column

Figure 1 shows a typical track of a liquid droplet in the linseed oil. As it follows from the figure, the steady motion of the droplet takes place from the very beginning of the deposition process due to the high viscosity of the carrier oil. The droplet moves at its terminal velocity towards the bottom of the column and settles within 20 s.

Following the simulation, a thin layer of ice crust was formed at the surface of the droplet just before it touched the bottom of the column. The crust is presented in Fig.2 together with the computational mesh. The CFD-analysis of the flow in the liquid core never revealed pressures above the Laplace pressure of the drop meaning the rapid ice formation did not destabilize or rupture the droplet and the crust. The shell is formed uniformly around the droplet, the solidification temperature is set at the ice front.
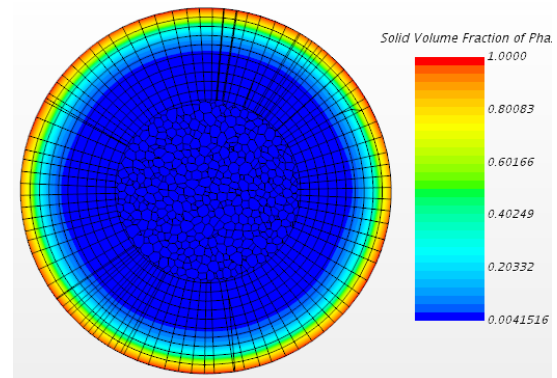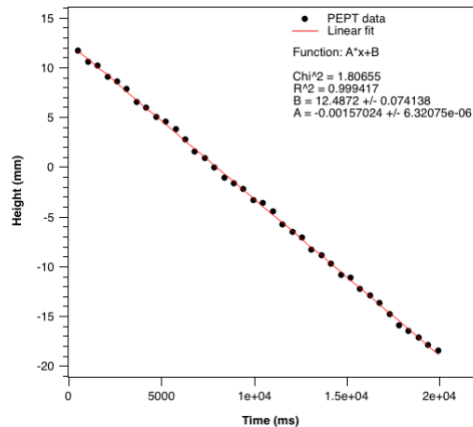
Figure 1. Tracking of 10 µl droplet of ^{68}Ga chloride solution falling in static column. Data sampling every 524.3 ms.

Figure 2. Computational mesh and volume fraction of ice in droplet at 15 s of the process.

4.2 Radioactive ice particles in mixer

In the experiments the formation of the ice particles in the beginning of the mixer operation was ensured by refreezing the dispensed droplets in a -80 ℃ freezer. The particle floated at the end of the track, so it can be assumed that it was frozen. After 3 mixing cycles of 40 s that happen within 10 minutes, the activity was found evenly distributed in the oil (by dividing the oil into several tubes and measuring the activity). This means the ice melted and the radioactive droplets were decomposed to smaller objects homogeneously distributed in oil.

Figures 3 – 4 depict a 40.2-sec track of a 0.5 µl ice particle in the mixer. The diameter of the ice particle is estimated 1012 µm, considering the ice density of 920 kg/m^3. The mixer blade was located at the top of the detector ring axial direction (z-axis top). The particle was positioned every 21 ms. As seen from the plot, the particle was lifted from the bottom of the column by a swirl originating from the mixer blade. Further, the particle was driven to the top of the FOV, being captured in a local vortex on the way to the top. A local increase of the particle flow velocity at 15 s of the process may be addressed to the swirl motion in the vicinity of the mixer; the second vortex of the track (Fig.3) confirms the assumption. After around 26 sec of mixer-on, the particle started to stay at the vertical top, floated with position and velocity fluctuations, and was not drawn downward or toward the mixer blade. The particle started to float at the vertical top at low speed after being expelled from the blade area.

The experimental data captured high-frequency oscillations of particle position and velocity. The particle tracks are visualised using Savitzky-Golay smoothing. The actual movement ranges of the ice particles in three directions are around 40 mm.
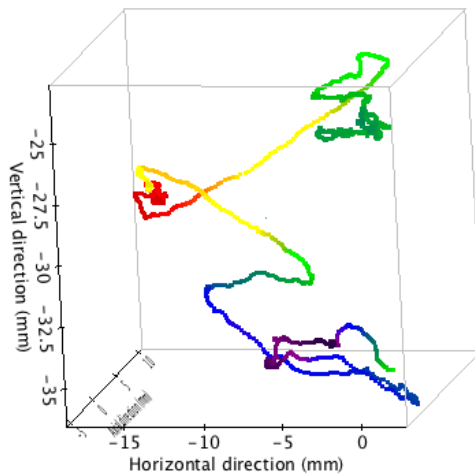
Figure 3. Track of 0.5 μl ice particle. The colour depicts Z-coordinate.
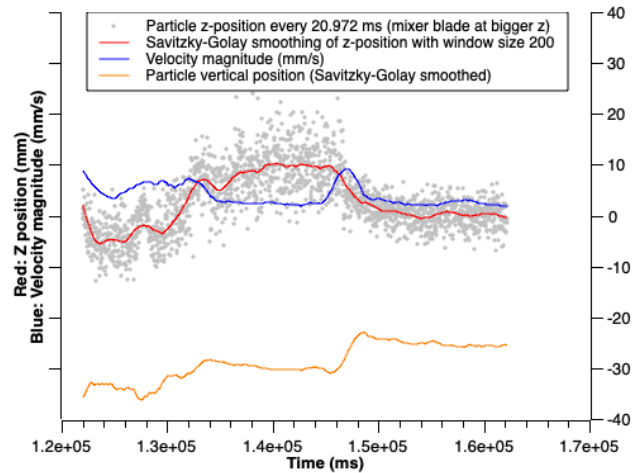
Figure 4. Velocity magnitude, vertical position and axial position (Z-coordinate) as a function of time for 0.5 μl ice particle.

5. Conclusion

In this study, we have demonstrated that the radioactive ice particles can be fabricated and can sustain the highly turbulent flow. It has been proved that our developed PEPT algorithms can be successfully applied to track the ice particle in turbulence. Therefore, the ice particle can be a feasible candidate as a bio-compatible PEPT tracer.

References

[1]   Bailey D L, Townsend D W, Valk P E and Maisey M N 2004 *Positron Emission Tomography: Basic Sciences* (London: Springer-Verlag)

[2]   Wiggins C, Santos R and Ruggles A 2016 A novel clustering approach to positron emission particle tracking *Nuclear Instruments and Methods in Physics Research Section A: Accelerators, Spectrometers, Detectors and Associated Equipment* **811** 18-24

[3]   Chang Y-F and Hoffmann A C 2015 A Lagrangian study of liquid flow in a reverse-flow hydrocyclone using positron emission particle tracking *Experiments in Fluids* **56** 4

[4]   Nicuşan A L and Windows-Yule C R L 2020 Positron emission particle tracking using machine learning *Review of Scientific Instruments* **91** 013329

[5]   Chang Y-F, Ilea C G, Aasen Ø L and Hoffmann A C 2011 Particle flow in a hydrocyclone investigated by positron emission particle tracking *Chemical Engineering Science* **66** 4203-4211

[6]   Balakin B V, Adamsen T C H, Chang Y-F, Kosinski P J, Hoffmann A C 2017 Non-invasive studies of multiphase flow in process equipment. Positron emission particle tracking technique. *Journal of Physics, Conference Series* **781** 012039

[7]   Hoffmann A C, Skorpen Å and Chang Y-F 2019 Positron emission particle tracking and CFD investigation of hydrocyclones acting on liquids of varying viscosity *Chemical Engineering Science* **200** 310-319

[8]   Cole K E, Buffler A, van der Meulen N P, Cilliers J J, Franzidis J P, Govender I, Liu C and van
        Heerden M R 2012 Positron emission particle tracking measurements with 50 micron tracers.
        Chemical Engineering Science **75** 235-42

[9]   Bergeron M, Cadorette J, Tetrault M-A, Beadoin J-F, Leroux J-D, Fontaine R and Lecomte R
        2014 Imaging performance of LabPET APD-based digital PET scanners for pre-clinical
        research *Physics in Medicine & Biology* **59** 661

[10]   Profir M, Moreau V and Melichar T 2020 Numerical and experimental campaigns for lead
        solidification modelling and testing *Nuclear Engineering and Design* **359** 110482

[11]   Crowe T C, Schwarzkopf J D, Sommerfeld M, Tsuji Y 2012 *Multiphase flows with droplets and
        particles* (Boca Raton: CRC Press)